# CHAPTER 2

# LITERATURE REVIEW

Interest in the chemistry of metal carboxylates has continued to grow through the years. Many workers have continued to investigate their fundamental properties, such as crystal structures, thermal properties and carboxylate bonding modes.

## 2.1 Structural review

Carboxylate ions are versatile ligands capable of existing simply as counter ions, or binding a metal in (a) monodentate, (b) chelating or (c) bridging modes. Bridging bonding is of special interest as it is known to give rise to a number of organo-metallo polymers and polynuclear molecules[1].

The structural chemistry of metal acetates has been the most widely investigated in the field of carboxylate chemistry. The acetate group often occurs as a bridging ligand linking two metal centres, leading to the formation of metal-metal bonds e.g. copper(II) carboxylates are commonly found as binuclear compounds. Documents dating as far back as the 1950's report the binuclear structure of copper acetate[2,3]. A review published by Robert Doedens in later years reported that the average Cu – Cu distance in a range of dimeric carboxylate complexes was found to be 2.619Å[4].

Van Niekerk and Schoening did some extensive work on the reactions of acetates with various transition metals. They found that zinc(II) acetate dihydrate exhibits bidentate chelate bonding, the least favoured and hence

rarest form of carboxylate bonding[5]. They reported that the formula units of this compound are linked by strong hydrogen bonds to form 2-D sheets, which accounts for the unique physical properties such as its softness and easy cleavage of crystals observed in this material.

Van Niekerk and Schoening's studies of cobalt(II) and nickel(II) acetate revealed that these compounds are isostructural, both exhibiting monodentate carboxylate bonding[6]. Each acetate group has one oxygen atom which forms a short bond to the metal atom and one non-bonded oxygen atom.

Van Niekerk and Schoening also supplied direct X-ray evidence that Cr – Cr bonds exist in chromium(III) acetate[7]. In subsequent years, Cotton and various co-workers also studied a variety of other carboxylates of chromium(III), all revealing metal – metal bonds[8,9,10]. Fig. 2.1 shows a paddle wheel arrangement of ligands around a $Cr_2^{4+}$ unit. Adjacent equatorial positions are usually occupied by bridging ligands.

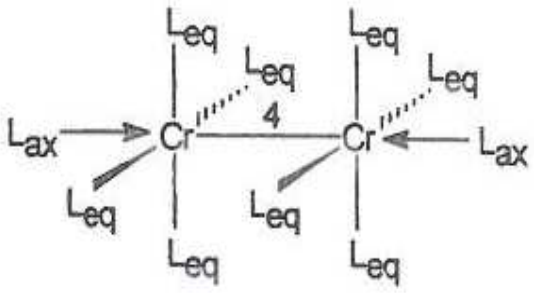


**Fig. 2.1** Paddle wheel type arrangement around the $Cr_2^{4+}$ unit[10]

Complexes where the acetate ligands act not only as chelating ligands but also as bridging ligands are exceptionally rare. However in the case of cadmium(II) acetate dihydrate, both acetate groups have been found to be bidentate chelating with one of the oxygen atoms also observed in a bridging position, forming a continuous cadmium-oxygen spiral network (Fig. 2.2)[11]. Extensive hydrogen bonding reinforces this Cd – O spiral and also links adjacent spirals.

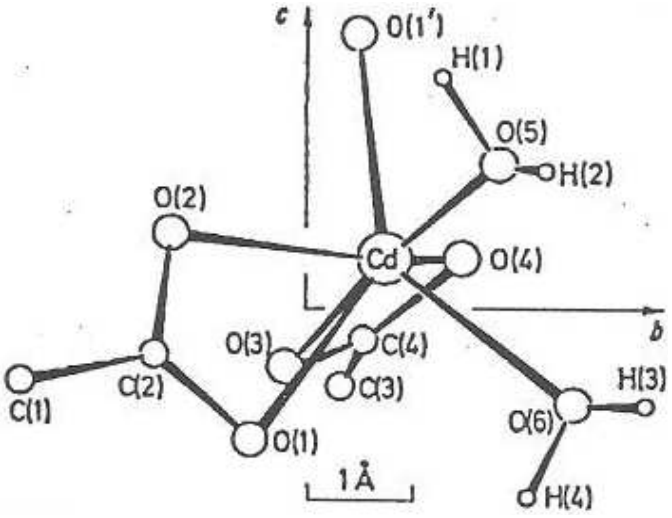


**Fig. 2.2** View of the cadmium coordination in cadmium acetate[11]

Zachariasen and co-workers studied sodium formate and confirmed that the formate group in the structure is ionic in nature[12]. This observation led them to suggest that all strongly electropositive elements will form ionic bonds with carboxylate moieties. This idea proved to be relatively accurate as more ionic compounds of alkali and alkaline earth metals were discovered. An exception however is lithium acetate, where the acetate group functions as a

monodentate ligand forming a short bond to the metal atom ($d_{Li-O}$ = 1.33 Å)[13].

Many of the formates of di-valent transition metals such as cobalt, nickel, copper, zinc, iron and manganese have been found to be isomorphous and isostructural[14]. Each metal atom is housed in an octahedral environment and these octahedra are bridged by a formate ion and hydrogen bonds. This network extends in a 3-D polymeric manner throughout the structure (Fig. 2.3).

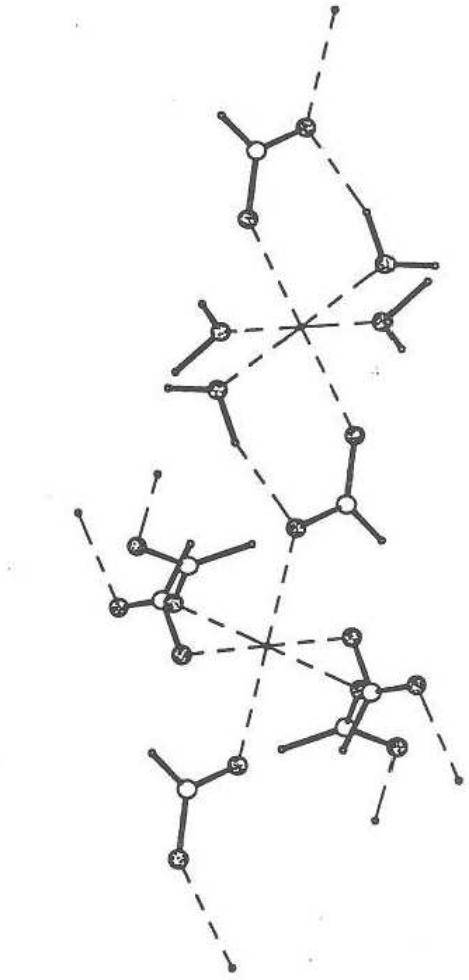

**Fig. 2.3** Stereographic view of the crystal packing in cobalt formate[14]

More recently, interest in the area of the structural chemistry of metal carboxylates has been focused on the rational design and construction of coordination polymers, which find applications in the field of supramolecular chemistry due to their interesting topologies[15]. Lanthanide co-ordination polymers have been synthesized and found to exhibit 2-D framework structures formed by the cross-linkage of carboxylate chains (Fig. 2.4)[15]. Alkaline earth metal carboxylates have also been shown to afford a bridge between liquid crystals and metal organic frameworks[16].

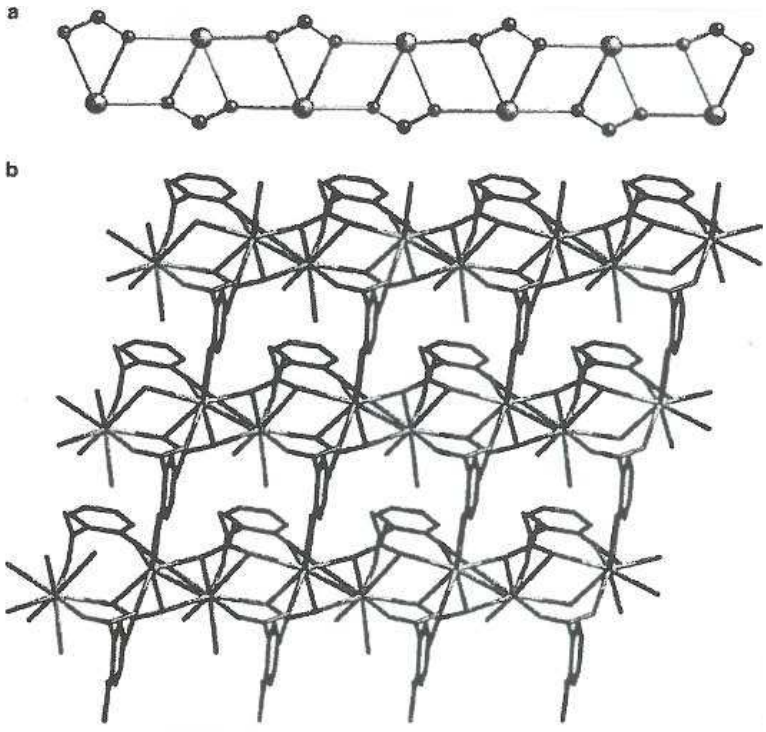


**Fig 2.4** (a) View of the La – O – La chain (b) 2-D framework structure formed by La – O – La chains[15]

In early 2008, a new orthorhombic polymorph of silver(II) malonate was synthesized[17]. The coordination environment of the silver atom, as well as the

bridging bonding mode of the malonate dianion, is shown in Fig. 2.5. The silver ion is five-coordinate, coordinating four oxygen atoms each in a *syn-anti* fashion. The familiar eight-membered $Ag_2(RCO_2)_2$ ring, characteristic of most silver(I) carboxylates, has an Ag – Ag distance of 2.977 Å. Puckered sheets of the crystals are connected to form a 3-D coordination polymer. This polymorph differs drastically from the monoclinic polymorph which was originally characterized in 1981[18].

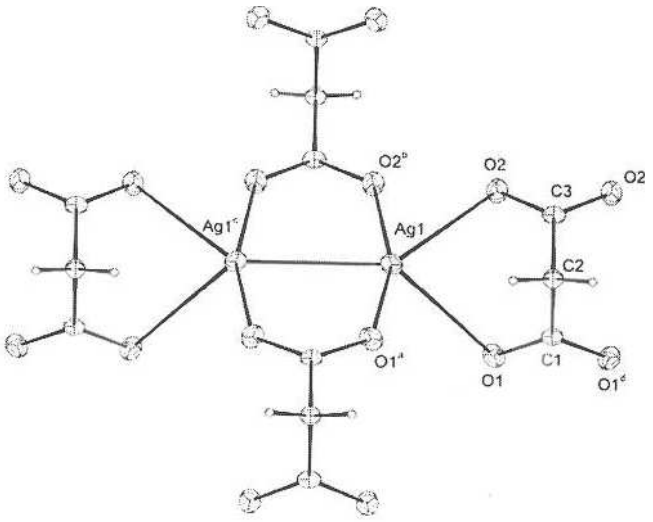


**Fig. 2.5** Structure of the $Ag_2(RCO_2)_2$ moeity in the orthorhombic polymorph[17]

### 2.2 Infrared spectroscopy

Sodium acetate has been widely studied with infrared spectroscopy. Being ionic in nature, this compound gives rise to a free unbound acetate ion when in solution. Fifteen infrared active fundamentals have been identified for the free acetate ion, of which the most important are the asymmetric and symmetric $COO^-$ stretching frequencies as these have been employed for

structural studies. Nakamoto showed that correlations exist between the separation of the asymmetric and symmetric $COO^-$ stretching frequencies (hereafter referred to as Δv) and the carboxylate bonding mode in carboxylate complexes[19]. This idea has spurred numerous exploratory studies in this area.

Ito and Bernstein studied the vibrational spectra of sodium acetate, oxalate and formate in solution[20]. They assigned all the major infrared active fundamentals for each ion and found that their results differed from earlier studies on the same compounds. Table 2.1 summarises their vibrational assignments for the acetate ion.

**Table 2.1** Vibrational assignments of sodium acetate[20]

| **Assignment** | **Type of vibration** | **Absorption maximum ($cm^{-1}$)** |
|---|---|---|
| $CH_3$ sym. str. | $A_1$ 1 | 2935 |
| $CH_3$ sym. def. | $A_1$ 2 | 1344 |
| $COO^-$ sym. str. | $A_1$ 3 | 1413 |
| C-C sym. str. | $A_1$ 4 | 926 |
| $CO_2$ sym. def. | $A_1$ 5 | 650 |
| C-H asym. str. | $B_1$ 7 | 3010 |
| $COO^-$ asym. str. | $B_1$ 8 | 1556 |
| $CH_3$ def. | $B_1$ 9 | 1429 |
| $CH_3$ rock | $B_1$ 10 | 1020 |
| $COO^-$ rock (in plane) | $B_1$ 11 | 471 |
| CH asym. str. | $B_2$ 12 | 3010 or 2981 |
| $CH_3$ def. | $B_2$ 13 | 1456 |
| $CH_3$ rock | $B_2$ 14 | 1052 |
| $COO^-$ rock (out of plane) | $B_2$ 15 | 621 |

The intense asymmetric $COO^-$ stretch is observed at 1578 $cm^{-1}$ and the weaker symmetric $COO^-$ stretch at 1414 $cm^{-1}$, which are separated by 164 $cm^{-1}$ (Δv). Δv for the oxalate and formate ions is 255 $cm^{-1}$ and 201 $cm^{-1}$ respectively.

Rao and co-workers studied the infrared spectra of some rare earth acetates to examine the metal-acetate bonding[21]. From their results (Table 2.2), it can be seen that Δv in the rare earth acetates varies from 105 – 130 $cm^{-1}$. It has been suggested that a divergence of Δv compared with the free acetate ion, is an indication of monodentate bonding[22]. Since these separations are smaller than that of sodium acetate, they concluded that the acetate group may be present as a monodentate ligand in these compounds. Furthermore, Δv in the rare earth acetates does not vary much with the metal and this led them to believe that the metal – oxygen bonds in all these cases were likely to be of similar strength.

**Table 2.2** Infrared frequencies of rare earth acetates[21]

| **Acetates** | **$V_{asym}$ ($cm^{-1}$)** | **$V_{sym}$($cm^{-1}$)** | **ΔV ($cm^{-1}$)** |
|---|---|---|---|
| Na | 1575 | 1422 | 153 |
| La | 1545 | 1440 | 105 |
| Pr | 1550 | 1440 | 110 |
| Nd | 1569 | 1439 | 130 |
| Sm | 1550 | 1420 | 130 |
| Gd | 1546 | 1420 | 126 |
| Dy | 1545 | 1418 | 127 |
| Lu | 1551 | 1412 | 139 |

Haywards and Edwards studied a series of transition metal acetates[23]. The results of their findings are summarized in table 2.3.

**Table 2.3** Infrared frequencies of some transition metal acetates[23]

| **Acetate** | **$V_{sym}$ ($cm^{-1}$)** | **$V_{asym}$($cm^{-1}$)** | **ΔV ($cm^{-1}$)** |
|---|---|---|---|
| Na | 1413 | 1556 | 143 |
| Mn(II) | 1410 | 1585 | 175 |
| Co(II) | 1405 | 1590 | 185 |
| Ni(II) | 1415 | 1600 | 185 |
| Cu(II) | 1420 | 1595 | 175 |
| Zn(II) | 1410 | 1550 | 140 |
| La(III) | 1410 | 1540 | 130 |
| Ce(III) | 1410 | 1550 | 140 |
| Mn(II).$4H_2O$ | 1400 | 1570 | 170 |
| Co(II).$4H_2O$ | 1395 | 1550 | 155 |
| Cu(II).$H_2O$ | 1410 | 1610 | 200 |
| Ni(II).$4H_2O$ | 1425 | 1550 | 125 |
| Zn(II).$2H_2O$ | 1405 | 1550 | 145 |
| La(III).$1.5H_2O$ | 1420 | 1560 | 140 |
| Ce(III).$1.5H_2O$ | 1415 | 1565 | 150 |

As previously stated, Δv values larger than that of the free acetate ion are associated with monodentate bonding. Although tetra-hydrated nickel, cobalt and manganese acetates are known to exhibit monodentate coordination, a small Δv is observed for these compounds.

In addition, the structure of dihydrated zinc acetate is known to be octahedral; the coordination to the metal consists of two oxygen atoms from two water molecules and four oxygens from chelating acetate groups[5]. However anhydrous zinc acetate shows an almost identical Δv to its hydrated counterpart. This means that the acetate groups could be tetrahedral with two chelating acetate groups, but an octahedral coordination by bridging and shared acetates is another possibility that cannot be ruled out.

Haywards and Edwards also disputed Rao's suggestions that the acetate groups in lanthanum acetate are monodenate[21], favouring the idea that the

high positive charge on the metal as well as its tendency to have high coordination numbers, would lead to chelating or bridging coordination.

These incongruencies led Haywards and Edwards to conclude that using Δv values to assess the mode of coordination of the acetate groups to metals is to be used with caution.

Grigorev studied the spectra of some bidentate acetates[24]. He correctly assumed that in chelating acetates the O-C-O angle would be smaller than in bridging acetates. He also considered the effect of changing the O-C-O angle without changing the force constant on the C-O frequencies and found from his calculations that increasing this angle should decrease the symmetric $COO^-$ stretching frequency and increase the asymmetric $COO^-$ stretching frequency, increasing Δv. The infrared spectra of the compounds of known crystal structures having only one type of acetate group support Grigorev's conclusions (Table 2.4). The chelating acetates show substantially smaller values of Δv then bridging acetates.

**Table 2.4** Infrared assignments in bidentate acetate groups[24]

| **Compound** | **C-O asym. str. ($cm^{-1}$)** | **C-O sym. str. ($cm^{-1}$)** | **Δv ($cm^{-1}$)** |
|---|---|---|---|
| **Chelating** | | | |
| $Zn(O_2CCH_3)_2.2H_2O$ | 1550 | 1456 | 94 |
| $Na(UO_2(O_2CCH_3)_3)$ | 1537 | 1472 | 65 |
| **Bridging** | | | |
| $Zn_4O(O_2CCH_3)_6$ | 1600 | 1441 | 159 |
| $Be_4O(O_2CCH_3)_6$ | 1639 | 1483 | 156 |
| $(Cu_2(O_2CCH_3)_4).2H_2O$ | 1603 | 1418 | 185 |

In an article reporting the infrared studies of two cobalt acetate compounds, Stoilova and co-workers proposed that a Δv separation of 105 – 140 $cm^{-1}$ is associated with monodentate bonding, 145 – 185 $cm^{-1}$ is associated with bidentate chelate bonding and 180 – 190 $cm^{-1}$ is associated with bidentate bridging bonding, based on their earlier work involving a comprehensive study of a number of metal acetates[25]. This study compared the spectra of cobalt acetate tetrahydrate (CATH) and cobalt acetate dihydrate (CADH) and revealed subtle differences between the two compounds (Fig. 2.6). Stoilova and his colleagues concluded that two different types of acetate groups are present in CADH as both the asymmetric and symmetric $COO^-$ stretching vibrations are split into two components, corresponding to each type of acetate group. They also surmised that the acetate groups in this compound were of a bidentate nature as opposed to the monodentate ligation known to occur in CATH.

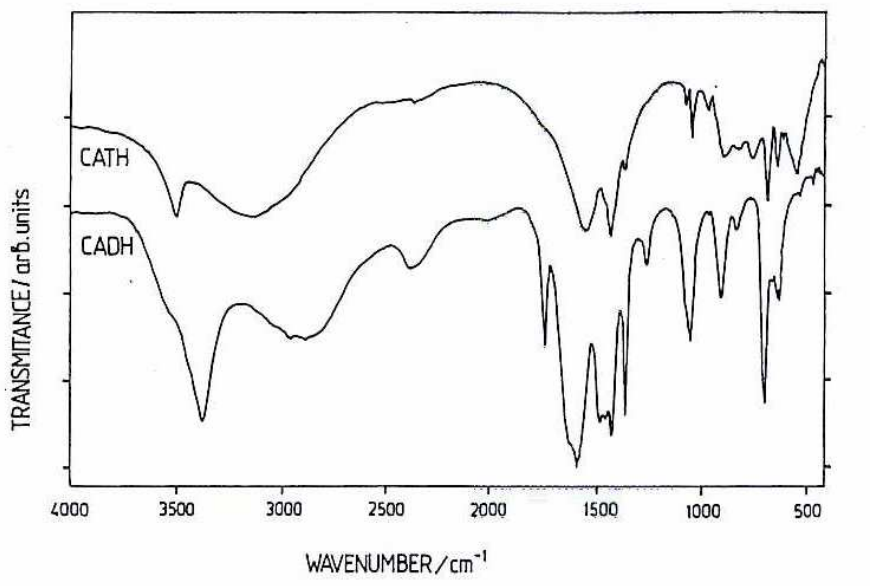


**Fig. 2.6** Infrared spectra of CADH and CATH[25]

## 2.3 Thermal analysis

There have been relatively few studies of the thermal decomposition behaviour of metal carboxylates. Metal formates, acetates and oxalates feature more dominantly than other carboxylates, possibly due to their potential use in catalyst preparations[26].

Judd and co-workers have investigated the thermal decomposition of the acetates of sodium, calcium, copper(II) and silver(I) using thermogravimetry (TG) and differential thermal analysis (DTA), together with analysis of the gaseous products formed during the decomposition process[27]. Their results suggest that the major organic product formed is either acetone or acetic acid depending on whether the final solid product is the metal oxide or pure metal. In the case of calcium, sodium and copper acetate, thermal decomposition yields the metal oxide, the former two proceeding via the formation of a metal carbonate intermediate. Silver acetate yields metallic silver as the final solid decomposition product.

Manabe and Kubo followed the decomposition of tetrahydrated magnesium acetate[28]. Their findings showed that the product is dehydrated in a single step to form an amorphous anhydride at ~160°C. A crystalline anhydride was obtained at 180 - 200°C (phase change occurred). This anhydride decomposed to give MgO at 300°C.

In their book, Mehrotra and Bohra indicate that the thermal decomposition of calcium acetate proceeds via the reaction[22]:

$$2Ca(O_2CCH_3)_2 \rightarrow CaCO_3 + 2(CH_3)_2CO\uparrow + CaO + CO_2\uparrow$$

Calcium carbonate and acetone are formed initially but upon further heating, calcium oxide and $CO_2$ are formed.

Barnes reported very similar results for the thermal decomposition of calcium propionate[29]. Two decomposition steps are observed; calcium propionate decomposes to the carbonate which subsequently decomposes to form CaO. Using GLC – MS coupled to the TG, they were able to accurately identify the gaseous components evolved during the decomposition of this compound and found that 3-pentanone accounted for over 90% of the total evolved gases. The overall decomposition reaction is:

$$2Ca(C_2H_5CO_2)_2 \rightarrow CaCO_3 + 2(C_2H_5)_2CO\uparrow + CaO + CO_2\uparrow$$

Rao and co-workers investigated the thermal decomposition of rare earth acetates as well lead(IV) and copper(II) acetate[21]. The anhydrous acetates are stable and decompose only above 400°C. The TG curves for selected rare earth acetates are shown in Fig. 2.7. The TG curves for all the rare earth acetates showed two stages: The first stage between 420 – 460°C corresponds to the decomposition of the anhydrous acetate to the oxycarbonate, $Ln_2O_3.CO_2$ and the second stage corresponds to the formation of the oxide, $Ln_2O_3$. In the case of lanthanum(III), samarium(III) and neodymium(III) acetate, DTA curves show that these compounds form normal carbonates prior to decomposition to $Ln_2O_3.CO_2$.

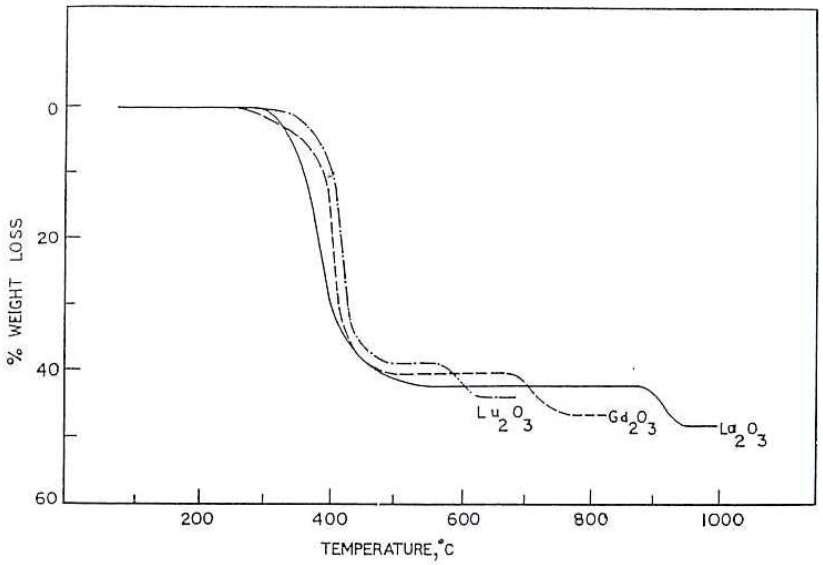


**Fig. 2.7** TG curves of selected anhydrous rare earth acetates[21]

Table 2.5 shows the TG analysis data of the rare earth acetates.

**Table 2.5** TG analysis data on the thermal decomposition of rare earth acetates, $Ln(CH_3CO_2)_3$[21]

| **Ln** | **Oxycarbonate formation temperature (°C)** | **Minimum oxide formation temperature (°C)** |
|---|---|---|
| La | 450 | 910 |
| Pr | 450 | 720 |
| Nd | 420 | 820 |
| Sm | 460 | 750 |
| Gd | 450 | 740 |
| Dy | 450 | 650 |
| Lu | 430 | 600 |

The minimum oxide formation temperature decreases markedly as the rare earth series is descended, possibly indicating that the coordination of the carbonate ion to the metal becomes stronger as the rare earth metal gets heavier.

The TG curve of lead tetra-acetate shows three distinct decomposition stages (Fig. 2.8) corresponding to the formation of diacetate, carbonate and oxide. Thus Rao and his co-workers suggested the following reactions for the decomposition of lead tetra-acetate:

$$Pb(O_2CCH_3)_4 \rightarrow Pb(O_2CCH_3)_2 + 2CH_3CO_2$$

$$2CH_3CO_2 \rightarrow CH_3CO_2CH_3 + CO_2$$

$$Pb(O_2CCH_3)_2 \rightarrow PbCO_3 + CH_3COCH_3$$

$$PbCO_3 \rightarrow PbO + CO_2$$

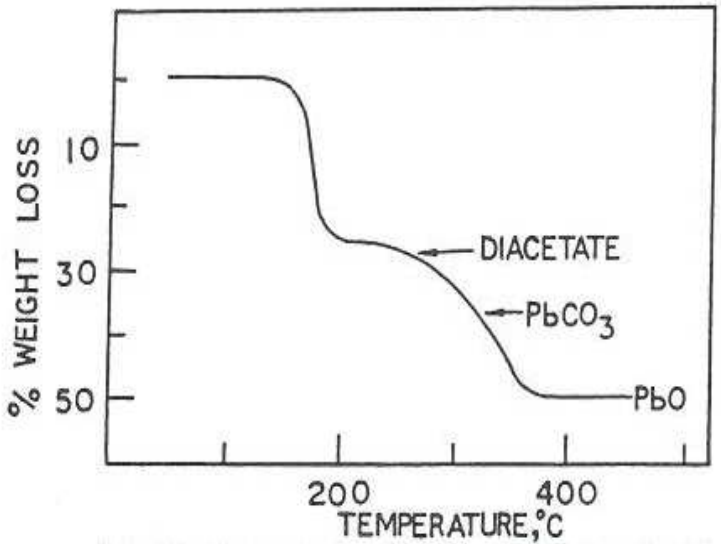


**Fig. 2.8** TG curve of lead tetra-acetate[21]

The decomposition of copper(II) acetate follows the reactions:

$$Cu_2(CH_3CO_2)_4.2H_2O \rightarrow Cu_2(CH_3CO_2)_4 + 2H_2O$$

$$Cu_2(CH_3CO_2)_4 \rightarrow 2CuO + 2CH_3COCH_3 + 2CO_2$$

Water, acetone and $CO_2$ are the main volatile products and the metal oxide is the final solid product.

Thermal decomposition studies of rare earth formates were carried out by Dabkowska[30,31]. Formates of lanthanum(III), cerium(III), praseodymium(III), neodymium(III), samarium(III), gadolinium(III) and dysprosium(III) lose crystal water at 25 – 30°C and are stable up to 300°C. The dihydrated formates of yttrium(III), holmium(III) and erbium(III) on the other hand, lose water at 100 – 110°C and are only stable up to 250°C. The final decomposition products are oxides of the general formula $Ln_2O_3$, with the exception of $CeO_2$ and $Pr_6O_{11}$. There is no evidence of oxycarbonate formation in the formates.

Thermal decomposition of selected anhydrous transition metal acetates under atmospheric conditions was investigated by Edwards and Hayward[23]. Their findings are summarized in Table 2.6.

**Table 2.6** Thermogravimetric results for transition metal acetates[23]

| | | 1st Decomposition stage | | | 2nd Decomposition stage | | | 3rd Decomposition stage | | |
|---|---|---|---|---|---|---|---|---|---|---|
| | | | Weight Change (%) | | | Weight change (%) | | | Weight change (%) | |
| | | Oxide | Obs. | Calc. | Oxide | Obs. | Calc. | Oxide | Obs. | Calc. |
| Acetate | | | | | | | | | | |
| Mn(II) | | MnO | 56.8 | 59.1 | $Mn_2O_3$ | 52.8 | 54.4 | $Mn_3O_4$ | 54.6 | 55.9 |
| Co(II) | | CoO | 54.8 | 57.7 | $Co_2O_3$ | 50.5 | 53.1 | $Co_3O_4$ | 51.9 | 54.6 |
| Cu(II) | | $Cu_2O$ + Cu | 61.8 | 62.1 | CuO | 56.0 | 56.2 | - | - | - |
| Zn(II) | | ZnO | 55.1 | 55.6 | - | - | - | - | - | - |
| Mo(II) | | $MoO_3$ | 31.2 | 32.7 | - | - | - | - | - | - |
| Ag(I) | | Ag | 35.8 | 35.4 | - | - | - | - | - | - |
| La(III) | | $La_2O_2CO_3$ | 41.5 | 41.5 | $La_2O_3$ | 48.4 | 48.4 | - | - | - |

The TG results for lanthanum(III) acetate are in good agreement with Rao's results discussed previously. The oxycarbonate, $La_2O_3.CO_2$, is completely formed at 480°C and is finally converted to $La_2O_3$ at 875°C. No oxycarbonate stage was observed in the TG curve of cerium(III) acetate, the only product being cerium(IV) oxide, formed at 500°C.

Both manganese(II) and cobalt(II) acetates decompose to the monoxides at ~ 350°C, which are then completely oxidized to the $M_2O_3$ phases at 600°C, followed by $M_3O_4$ stages at 950°C.

Copper(II) acetate starts to decompose at 230°C to a mixture of copper metal and copper(I) oxide, both being completely oxidized to copper(II) oxide by 535°C.

Zinc(II) and molybdenum(II) acetates decompose to ZnO and $MoO_3$ at 350 and 280°C respectively as the sole products. Silver(I) acetate produces only silver metal by 280°C, with no evidence of oxide formation at lower temperatures.

Rai and Parashar reported thermogravimetric analysis of some higher carboxylate derivatives of chromium(III) [32]. The DTG curves of these compounds indicated that two-step decomposition occurred. These tricarboxylates are stable up to 210°C and then slowly start decomposing, forming chromium oxycarboxylate compounds, ketones and $CO_2$. The ketones which form in the process also undergo decomposition with atmospheric oxygen to yield $CO_2$ and $H_2O$. In the second stage, the oxycarboxylates undergo further decomposition above 380°C to form chromium trioxide and the corresponding ketones, which again decompose rapidly in air to yield $CO_2$ and $H_2O$.

A comprehensive study of a series of metal formates, including sodium, potassium, calcium, barium and selected d-block metals such as cobalt, zinc, nickel and iron, reveals that thermal decomposition of the formates proceeds via two different pathways[33]. The first group of formates, i.e. sodium,

potassium, calcium and barium, thermally decompose to carbonate before finally decomposing to metal oxide. Although this observation is not uncommon for these metals (recall studies of calcium acetate and propionate revealed similar findings), what is unique is that three of these salts, sodium, potassium and barium formate, form a second intermediate when heated under vacuum. The author's hypothesis is that this transformation is oxalate formation:

$$2HCOO^- \rightarrow C_2O_4^{-2} + H_2$$

$$C_2O_4^{-2} \rightarrow CO_3^{-2} + CO$$

Intermediate carbonate formation is absent in the remaining formates, magnesium, copper(II), zinc(II), cobalt(II), nickel(II), manganese(II), iron(II) and cadmium(II). These decompose to form metal oxide at markedly different temperatures. Table 2.7 shows the TG data for the transition metal formates in air.

**Table 2.7** TG data for transition metal formates in air[33]

| **Formate** | **Dehydration temp. (°C)** | **Decomposition temp. (°C)** | **Final product(s)** |
|---|---|---|---|
| Cu | 90 | 150 | $CuO + Cu_2O$ |
| Zn | 90 | 145 | ZnO |
| Cd | 80 | 150 | CdO |
| Fe | 70 | 120 | $Fe_2O_3$ |
| Co | 90 | 190 | $Co_3O_4$ |
| Ni | 100 | 200 | NiO |
| Mn | 80 | 160 | $Mn_3O_4$ |

Bassi et al. examined the thermal decomposition of cobalt(II), nickel(II), copper(II) and zinc(II) propionate[34]. Zinc(II) and cobalt(II) propionate

decompose at 325 and 300°C respectively, both being rapidly oxidized to the MO stage by ~350°C. Nickel(II) and copper(II) propionate start decomposing at slightly lower temperatures, 285 and 255°C respectively, to yield NiO at 285°C and CuO at 255°C. Fig. 2.9 shows the TG and DTG curves of zinc(II) propionate monohydrate.

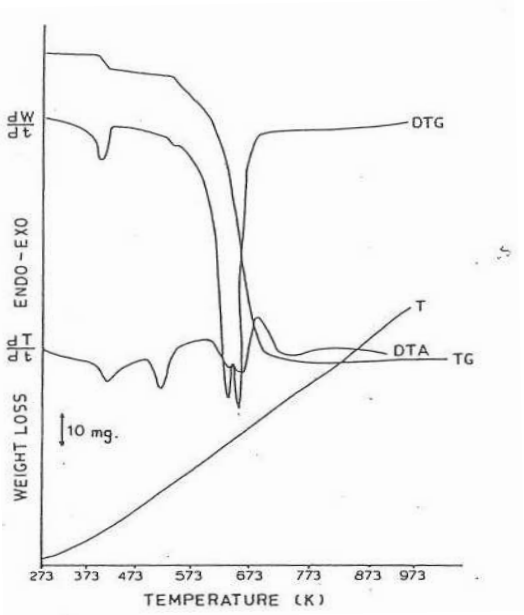


**Fig. 2.9** Simultaneous TG and DTG curves of zinc(II) propionate monohydrate[34]

Metal oxalates have also found themselves to be the subject of systematic studies. Galwey and co-workers recently published an article comparing the thermal reactivities of some transition metal oxalates in various atmospheres[35]. Two trends were identified from their work: (1) In inert and reducing atmospheres, the decomposition temperature of the salts increases with the rise in enthalpy of formation of the metal oxide thus implying that the strength of the metal – oxygen bond is the parameter that determines the stability of the oxalates. (2) The drop in decomposition temperatures from

values for reactions in inert/reducing atmospheres to those in oxidizing atmospheres increases with the difference in formation enthalpy between MO and the other participating oxide ($M_3O_4$ or $M_2O$), implying that the change in metal valence tends to promote the reaction.

Table 2.8 summarises the results obtained in various atmospheres for the metal oxalates.

**Table 2.8** TG data for different metal oxalates at 10°C/min[35]

| **Gas** | | **Mn(II)** | **Fe(II)** | **Co(II)** | **Ni(II)** | **Cu(II)** | **Zn(II)** |
|---|---|---|---|---|---|---|---|
| **$N_2$** | **ML%** | 50.2 | 55.4 | 55.4 | 59.4 | 56.9 | 48.0 |
| | **$T_{max}$ (°C)** | 418 | 201.6<br>264<br>351 | 191.5<br>316.9 | 229.1<br>367.6 | 299.8 | 411.8 |
| **$CO_2$** | **ML%** | 50.4 | 56.6 | 55.5 | 60.0 | 56.0 | 48.0 |
| | **$T_{max}$ (°C)** | 425 | 204.7<br>284<br>384<br>411.4 | 190.4<br>340.1 | 236.7<br>375<br>392 | 309.6 | 421.6 |
| **$H_2$** | **ML%** | 51.0 | 69.3 | 68.0 | 68.1 | 59.6 | 48.1 |
| | **$T_{max}$ (°C)** | 409 | 69.3<br>208.8<br>258.7<br>407.3 | 68.0<br>190.4<br>359.5<br>370.7 | 258.7<br>348.3 | 283.5 | 405.3 |
| **Air** | **ML%** | 46.4 | 55.8 | 56.0 | 60.3 | 54.6 | 48.2 |
| | **$T_{max}$ (°C)** | 299 | 204.5<br>231.4 | 199.2<br>303.1 | 270.9<br>340.1 | 307.1 | 406.9 |

Thermal decomposition of some transition metal malonates and succinates has been studied using a combination of thermal techniques as well as XRD, SEM and Mőssbauer[36]. This work reveals that after dehydration, the

anhydrous metal malonates and succinates decompose directly to their respective metal oxides in the temperature ranges 310 – 400 and 400 – 525°C, respectively. SEM images reveal that the oxides obtained are nanosized. The thermal stability of succinates was found to be higher than that of the respective malonates (Fig. 2.10).

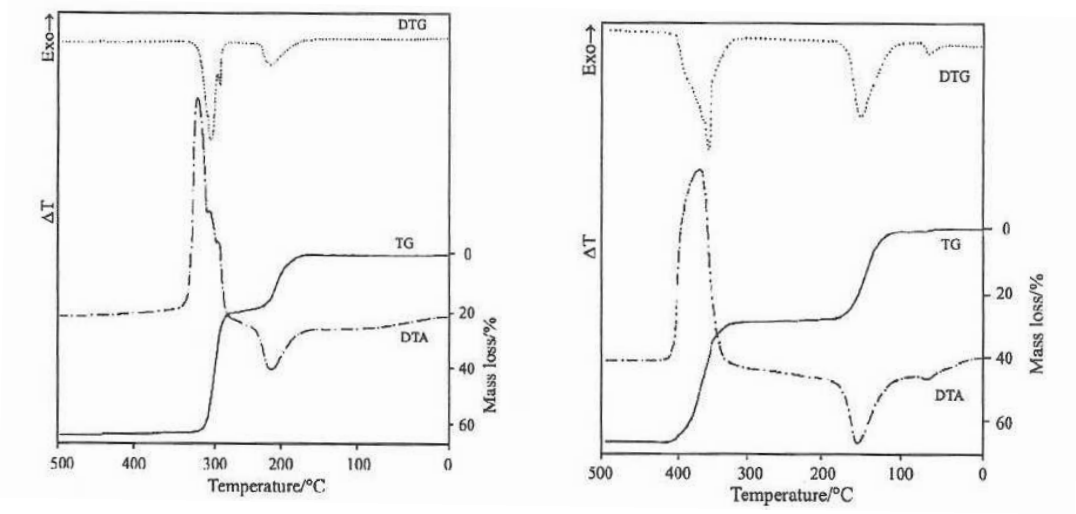


**Fig. 2.10** Simultaneous TG – DTG – DTA curves of (a) cobalt malonate and (b) cobalt succinate[36]

Leicester and Redman reported the thermal decomposition of nickel and cobalt salts of aliphatic acids, in particular the acetates[37]. They found that these salts decompose via primary cleavage into metal oxides. Nickel salts also yields nickel carbide. Kinetic studies of nickel acetate reveal that the salt decomposes via an autocatalytic mechanism, however kinetic studies of cobalt acetate could not be effectively carried out as the authors found that these salts cake when heated resulting in non-reproducible results. It was also noted that cobalt compounds tended to decompose to metallic cobalt when

heated too rapidly or in a limited air supply. $CO_2$, acetic acid and ketones were found to the major organic decomposition products.

The thermal analysis of cobalt oxalate, formate and acetate was carried out with simultaneous TG – DTG – DTA measurements in air and argon[38]. The decomposition of the studied compounds occurs in several stages, the first of which is always dehydration in both air and argon. $Co_3O_4$ is the final decomposition product of all three compounds in air. In argon, a mixture of CoO and Co is obtained for the formate and oxalate and only CoO for the acetate. The authors this concluded that selected cobalt carboxylates could be used as precursors to obtain cobalt metal powder.

In a more detailed study, the non-isothermal decomposition of cobalt acetate tetrahydrate was explored by means of TG, DTA and DSC techniques[39]. The complete course of decomposition of this compound is described by six thermal events. Event I (30 – 140$^o$C) is attributed to partial dehydration of the tetrahydrate to form a monohydrated species. Event II (168 – 195$^o$C) is signified by a small mass loss but high enthalpy value and is believed to be a bulk restructuring of the monohydrate. Event III (223 – 251$^o$C) is an exothermic process accompanied by a small mass loss and is assigned to the formation of an intermediate compound identified as acetyl cobalt acetate. Event IV (250 – 290$^o$C) is an endothermic process and infrared results suggest that a second intermediate, cobalt acetate hydroxide, is formed. Event V (315 – 360$^o$C) is accompanied by a large mass loss (31%) and represents the autocatalytic decomposition of the adsorbed acetate and other related compounds on the surface of cobalt oxide. Event VI (370 – 390$^o$C) is an exothermic process accompanied by no mass loss and is thought to be the recrystallization of the CoO produced.

There are few accounts of the thermal behaviour of long chain metal carboxylates. One of these reports, by Wood and Seddon was published on stearates and dodecanoates in the 1980's[40,41,42]. The authors reported that chromium tends to form –OH substituted stearates, $CrSt_2OH$ and $CrSt(OH)_2$ (St = stearate). DTG curves for these compounds show that stearic acid is released in two distinct stages. In other studies, Wood and Seddon examined the thermal decomposition of several metal dodecanoates. Their results suggest that the decomposition mechanisms of these large molecules is quite complex, as evolved gas analysis showed that a number of ketones containing from 3 to 18 carbon atoms are evolved during this process. The final products of decomposition are metal oxides for chromium, zinc, copper and nickel and metal carbonates for calcium and sodium.

More recent advances in this field include studies of the thermal decomposition of bimetallic carboxylates, such as manganese(II)bis(oxalato)cobaltate hydrate, iron(II)bis(oxalato)cobaltate pentahydrate and copper(II)bis(oxalato)cobaltate trihydrate[43].

**2.4 References**


[1] P. C. Junk, C. J. Kepert, L. Wei-min, B. W. Skelton and A. H. White, *Aust. J. Chem*., **42** (1999) 437

[2] J. N. Van Niekerk and F. R. L. Schoening, *Nature*, **171** (1953) 36

[3] J. N. Van Niekerk and F. R. L. Schoening, *Acta Crystallogr*., **6** (1953) 227

[4] R. J. Doedens, *Prog. Inorg. Chem*., **21** (1976) 209

[5] J. N. Van Niekerk, F. R. L. Schoening and J. H. Talbot, *Acta Cryst*., **6** (1953) 720

[6] J. N. Van Niekerk and F. R. L. Schoening, *Acta Cryst*., **6** (1953) 609

[7] J. N. van Niekerk, F. R. L. Schoening, *Acta Cryst*., (1953)

[8] F. A. Cotton and G. W. Rice, *Inorg. Chem*., **17** (1978) 2004

[9] F. A. Cotton, E. A. Hillard, C. A. Murillo and H. Zhou, *J. Am. Chem. Soc*., **122** (2000) 416

[10] F. A. Cotton and G. Schmid, *Inorg. Chim. Acta*, **254** (1997) 233

[11] W. Harrison and J. Trotter, *J.C.S Dalton*, 956

[12] W. H. Zachariasen, *J. Am. Chem. Soc*., **62** (1940) 1011

[13] V. Amirthalingam and V. M. Padmanabhan, *Acta Cryst*., **11** (1958) 896

[14] A. Kaufman, C. Afshar, M. Rossi, D. E. Zacharias and J. P. Glusker, *Struct. Chem.*, **4** (1993) 191

[15] C. Qin, X. Wang, E. Wang and L. Xu, *Inorg. Chim. Acta*, **359** (2006) 417

[16] R. W. Corkery, *Curr. Opinion in Coll. & Interface Sci*., **13** (2008) 288

[17] J. Prakashareddy and B. M. Foxman, *J. Mol. Struc*. (2008) doi: 10.1016/ J.molstruc. 2008.04.034

[18] F. Charbonnier, R Faure and H. Loiseleur, *Rev. Chim. Miner*., **18** (1981) 245

[19] K. Nakamoto, *Infrared and Raman Spectra of Inorganic and Coordination Compounds*, Wiley, New York (1978)

[20] K. Ito and H. J. Bernstein, *Can. J. Chem*., **34** (1956) 170

[21] K. C. Patil, G. V. Chandrashekhar, M. V. George and C. N. R. Rao, *Can. J. Chem*., **46** (1968) 257

[22] R. C. Mehrotra and R. Bohra, *Metal Carboxylates*, Academic press, New York (1983)

[23] D. A. Edwards and R. N. Hayward, *Can. J. Chem*., **46** (1968) 3443

[24] A. I. Grigorev, *Russ. J. Inorg. Chem*., **8** (1963) 409f

[25] Zh. Nikolov, G. Georgiev, D. Stoilova and I. Ivanonv, *J. Mol. Struc*., **354** (1995) 119

[26] D. L. Trimm, *Design of Industrial Catalysts, Chemical Engineering Monograph II*, Elsevier, Amsterdam (1980)

[27] M. D. Judd, B. A. Plunkett and M. I. Pope, *J. Therm. Anal*., **6** (1974) 555

[28] K. Manabe and T. Kubo, *Chem. Abstr*., **67** (1967) 78612d

[29] P. A. Barnes, G. Stephenson and S. B. Warrington, *J. Therm. Anal*., **25** (1982) 299

[30] M. Dabkowska, *Chem. Abstr*., **87** (1977) 94759q

[31] M. Dabkowska, *Chem. Abstr*., **87** (1977) 94760u

[32] A. K. Rai and G. K. Parashar, *Thermochim. Acta*, **29** (1979) 175

[33] P. Baraldi, *Spectrochim. Acta*, **35A** (1979) 1003

[34] P. S. Bassi, H. S. Jamwal and B. S. Randhawa, *Thermochim. Acta*, **71** (1983) 15

[35] M. A. Mohamed, A. K. Galwey and S. A. Halaway, *Thermochim. Acta***, 429** (2005) 57

[36] B. S. Randhawa and K. Gandotra, *J. Therm. Anal*., **85** (2006) 417

[37] J. Leicester and M. J. Redman, *J. Appl. Chem*., **12** (1962) 357

[38] E. Ingier-Stocka and A. Grabowska, *J. Therm. Anal*., **54** (1998) 115

[39] M. A. Mohamed, S. A. Halaway and M. M. Ebrahim, *J. Therm. Anal*., **41** (1994) 387

[40] J. A. Wood and A. B. Seddon, *Thermochim. Acta*, **53** (1982) 235

[41] A. B. Seddon and J. A. Wood, *Thermochim. Acta*, **106** (1986) 341

[42] A. B. Seddon and J. A. Wood, *Thermochim. Acta*, **118** (1987) 253

[43] N. Deb, *J. Anal. Appl. Pyrolysis*, **78** (2007) 24